EXPERIMENTAL AND NUMERICAL STUDY OF GaAs SINGLE CRYSTAL GROWTH IN THREE – DIMENSIONAL PSSM; BY HORIZONTAL BRJDGMAN METHODS

OGBONDA, CLEMENT
Department of Physics
Ignatius Ajuru University of Education
Rumuolumeni, Port Harcourt

And

WAGBARA EVEREST
Department of Physics
Ignatius Ajuru University of Education
Rumuolumeni, Port Harcourt

Abstract

Experimental and Numerical study in distribution of impurities in GaAs single crystal growth has been carried out by horizontal Bridginan method. In addition, transport phenomena namely; momentum, heat and concentration gradient were performed. Simulation results show that ,in 3 - dimensional Pseudo Steady State Model (PSSMJ), the interface is less curved, hence the flow intensity is weaker, temperature in the center area of the growth cell continues to decrease during the process of crystal growth. These results are in good agreement with our experimental data, which demonstrates that the finite element model can successfully predict the temperature field variations in the growth cell.

Keywords: Horizontal Rridgman, Single crystal Growth, Psuedo Steady State, Finite Element Method, Newton-Raphson method.

Introduction

Crystal growth involves a variety of research fields ranging from surface Physics, crystallography and material science to condense matter Physics. lt has been studied extensively some hundred years ago, crystal growth still plays an important role in both theoretical and experimental research fields as well as applications(Shockley, 1993). Single crystalline material has played an important role in miniaturization with consequent price reduction and higher efficiency of solid state equipments. Fisher, et al (2013), worked on the principles of crystal growth of intermetallic and oxide compounds from molten solutions with an emphasis on the fundamental principles governing underlying phase equilibria and phase diagrams of multi-component system. They found that at constant temperature and pressure for a binary mixture, equilibrium phases minimize the Gibs free energy (G) of a system, G=E + PV-TS = H — TS. The free energy of two phases cross, there is a phase transition. Melting transitions involves a latent heat and are therefore always first order. It was also found that phase separation in mixture of two and more components for binary system reveals that there are only a limited number of distinct phase in equilibrium for any given composition or temperature. The Gibbs phase rule reveals the number of available degrees of freedom (F) left to the system — that is the number of intensive parameter independently varied while still maintaining equilibrium. The study also revealed that solidification sequence is used to grow crystals from molten solutions, by considering the solidification sequence as a melt is slowly

cooled, using schematic binary phase diagram. Congruently melting compound, cooling a stiochiometric melt results in a single phase solid sample.

Ciszek and Wang (2000), worked silicon float-zone crystal growth as a tool for the study of defects and impurities. In this study, defects and impurities such as grain size, dislocations, swirl defects, and fast-cooling defects. The impurities studies focused on hydrogen, nitrogen, iron (H, N, Fe) and interactions between Fe and gallium (Ga). The study revealed how the effect of defect, impurity, and growth parameter affects the silicon(Si). It shows that the present of impurities and defects during the growth of Si crystal is paramount, the life time of Si is reduced, presence of dislocations and grain boundaries.

Kirkpatrick (1975), worked on a review of crystal growth from the melt: The study reviewed four aspect of crystal growth theory: the nature of rate controlling process, the mechanism controlling molecular attachment onto growing crystal surface, the nature of the crystal-melt interface, and stability of planar interfaces relative to cellular interfaces, It was shown that the rate at which a crystal grow can be controlled by any of the three factors: diffusion in the melt (either long or short range), flow latent heat away from the growing crystal surface, or reactions at the crystal-melt interface.

Blagden (2005), carried out a study Monitoring Polymorphic Transformations in Solution. In his study, he applied diffraction techniques to the study of crystallization from solution is a way to study the process of crystallisation under different solvent conditions, super saturation and cooling regimes. Kaci, et al (2005), in the same manner, investigated Optical and Morphological Properties of Lead Sulphide (PbS) thin Films. Experimentals result showed that the shape of the product depended on the initial reactants.

Qubbaj et al (2002), worked on the numerical modeling of a turbulent gasjct flame in a swirling air stream. Anumerical computation were carried out using the commercially avoidable software package, on the numerical simulation of a turbulent natural gas jet diffusion flame at a Reynolds number of 9000 in a swirling air stream. The results showed the generation of two recirculation regimes induced by swirling air stream, which account for such effects.

Similarly Falster (2012), investigated the defect control in silicon crystal growth and water processing. Accurate control of the defective silicon crystals and wafers is a subject of immense importance to both the silicon and integrated circuit (IC) industries. They revealed that, crystal growth has problems of intrinsic point defect concentration and reaction control in the growth crystals including effects of impurities and the uses of vacancy concentration profiles installed into silicon wafcr in order to achieve ideal oxygen precipitation performance.

In the same manner, Hung (2009), worked on the Epitaxial crystal growth. In this study a numerical simulation of the spiral growth using a phase-field formulation of the burton-cabrera-frank model. The result shows that real crystals are not perfect, they contain dislocations which are crystallographic defects in the structure of the crystal lattice as depicted, the presence of dislocations influences the mechanism of crystal growth. If dislocations are present in the crystal lattice of the substrate, they provide a way of controlling the growth as are source of new steps where atoms are incorporated to, hence, the growth proceeded at lower temperatures and super saturations.

Nollet, et al (2006), have carried out an experimental study of polycrystalline growth from an adverting supersaturated fluid in a model fracture. The result shows that, average growth rate of the crystals is influenced by growth competition and the depletion of the solute

along fracture length and growth competition is controlled by crystallographic orientation, crystal size and crystal location. In addition, the growth rate of an individual crystal facet also shows variations depending on the facet index, facet size and flow velocity. These variations can influence the morphology of the grain boundaries and the microstructures. It was observed that, the measured growth rates have a much larger range than predicted by alum single-crystal growth kinetics, this is due to the combined effect of the facet index and the crystal size.

Riedi and Wendrock (2014), studied the reliability of high resolution electron backscatter diffraction determination of strain and rotation variation using phase-only and cross correlation. . It is shown that, the Fourier filter width has a major impact on the strain results, at high noise level a small filter width has to be applied for obtaining maximum precision, and the influence of degree of overlap of the regions of interest positioned in patterns is less important. For both rotation and bending experiments the cross correlation variant yields a smaller standard deviation with respect to phase-only correlation, in particular for elevated noise level, this difference is attributed to the strong propagation of noise effects in the course of phase-only correlation function.

Wang et al (2014), carried out a study on a four-element sensor array consisting of asymmetric distributed — feedback fiber laser. In this study a sensor array system is formed by arranging four asymmetric distributed- feedback fiber laser (DFBFL) in ascending order according to their slop efficiencies was proposed. It is found from the result. that the relaxation oscillation frequency of a certain distributed-feedback fiber laser (DFB-FL) was relevant to its relative position in the array. And the relativeintensity noise (RIN) of a certain DFB-FL was always affected by the other elements in the array, which was not dependent on the order of their arrangement.

Kakimoto (2013), studied the development of crystal growth technique of silicon by the Czochralski method. In this study a reflector was used for separation of the heating and cooling areas in the furnace enabling it to speed up crystal growth. The result shows defect formation of heat and mass transfer during the silicon single crystal growth by the Czochralski method. A reflector is used to separate heating and cooling areas in the furnace and increase crystal growth velocity. Transverse magnetic fields used in a large-scale silicon Czochralski furnace allow for control of the melt-low. The Transverse magnetic Czochralski Zone (TMCZ) system can allow for the modification of important parameters, for the formation of point defects such as vacancies and interstitials.

Fedyushkm and Bourago (2001), investigated the influence of vibrations boundary layers in Bridgman crystal growth. In their study the finite element code ASTRA the effect of vibration on the melt flow in Bridgman crystal growth is investigated for the earth and space gravity conditions. It was found that by means of post-processing the instant thermo-mechanical fields found in numerical integration of Navier-Stokes problem. The structure of average vibrational flow (AVF) depends on the physical frequency/amplitude values. The frequency of vibrations (vibrational Reynolds number)influences essentially on the AVF structure. Numerical results also showed that the direction of the vibrations significantly decrease the width of interfacial boundary layers in Bridgman crystal growth with submerged vibrator. It is shown that for normal and low gravity conditions the vibrations can decrease the width of boundary layers and increase the boundary temperature gradients. this intensify heat and mass transfer near the solid-liquid interface and increase the rate of crystal.

Grishechkin and Kapshai (2014), carried out study on the couples — states of relativistic two-particle systems with energy dependent single boson exchange potentials. numerical solutions of the equations of quantum field theory was used. The result shows that the transition frequencies of the system from the first excited state to the ground state and the decay widths of the bound state of two particles into two photons were interrelated. The obtained energy spectra and decay widths agrees with the experimentally measured values for positronium when compared together.

Fang, et al (2013), studied the crystal cracking analysis and three-dimensional effects during kyropoulos sapphire growth. From the result, Cracks are observed in the grown ingot that significantly reduces industrial productivity, thermal stress and three-dimensional effects during the stable growth of sapphire crystal. It is found that locally induced thermal stress around the shoulder of the crystal is the largest. However, thermal stress is not fully responsible for the cracks.

Wang, et at (2013), investigated the crystal growth, structure and spectroscopic studies of a novel organic single crystal: The result of the study revealed that the single crystal X-ray diffraction has shown that LLNP belongs to the orthorhombie crystallographic system with space group P222,. The functional groups and vibrational frequencies of the crystal have been identified using IR and Raman spectra.

Ezema (2004), carried out a study on the method of decomposition of zinc oxide (ZnO) for production of thin film, reported that thin film of ZnO have been used but its preparation techniques have been restricted to sputtering, vacuum evaporation, chemical vapour deposition, spray prolysis, molecularbeam epitaxy, solgel and pulse laser.

An important aspect of this has been a significant improvement in the ability to model the complex thermal and concentration gradient dynamics of Gallilium Arsenide crystal growth. The present work is considered to deal with experimental and numerical study of GaAs single crystal growth in three — dimensional PSSM by horizontal bridgeman methods.. The governing boundary layer equations are solved by an implicit finite-difference scheme of Newton-Raphson method type with various parameters Pr,Sc,Gr, and Pe. In order to check the accuracy of our numerical results, the present results are compared with the available results of Arakawa, (1966); Hossian (2002). For non-uniform surface heat flux and Lin (1976) for uniform heat flux and are found to hem excellent agreement.

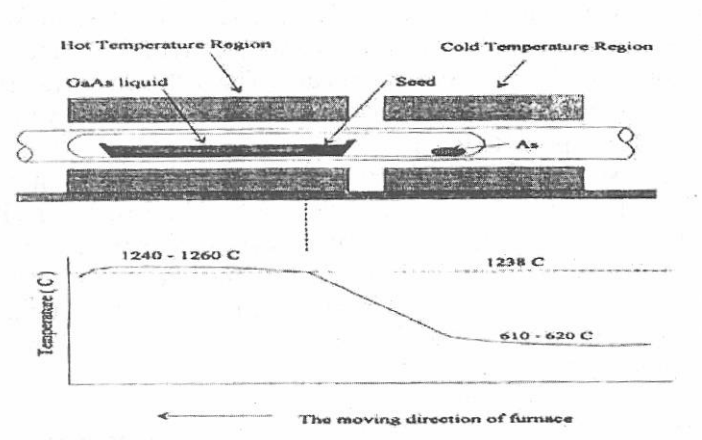

Figure I. The Schematic Diagram of HB Furnace Growing GaAs.

Mathematical Analysis

Assuming the boat in Figure 1. as 3-dimensional rectangular parallelepiped, and also the wall of the boat which enclose melt and crystal is taken to be sufficiently thin. (see Fig 2). In a 3-dimensional PSSM, velocity has three components, i.e

$\vec{u} = (u, v, w)$ The equations in the melt are now

Assuming the boat in Figure 1. as 3-dimensional rectangular parallelepiped, and also the wall of the boat which enclose melt and crystal is taken to be sufficiently thin. (see Fig 2). In a 3-dimensional PSSM, velocity has three components, i.e

$\vec{u} = (u, v, w)$ The equations in the melt are now

$$\nabla \cdot \vec{V} = 0 \qquad \vec{V} = (u, v, w) \tag{1}$$

$$\vec{V} \cdot \nabla \vec{V} = -\nabla p + \nabla^2 \vec{v} - Gr\, T \vec{e}_x \tag{2}$$

$$Pr \vec{V} \cdot \nabla T = \nabla^2 T \tag{3}$$

$$Sc \vec{V} \cdot \nabla C = \nabla^2 C \tag{4}$$

$$T_{interface} = T_{melting\ point} \tag{5}$$

The energy equation in the crystal is

$$Pe\ \vec{e}_x . \nabla T = r \nabla^2 T$$

The boundary condition for velocity field is no-slip condition at the wall and at the interface

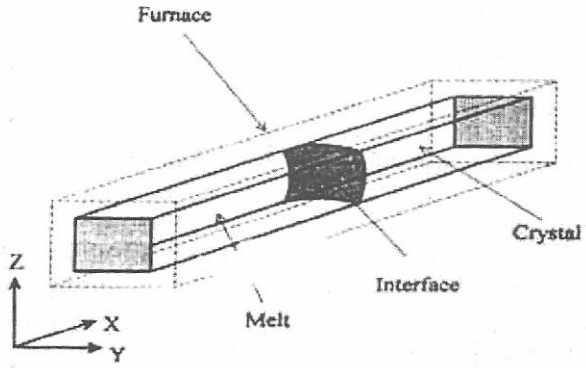

Figure 2. The Simplified Diagram PSSM of RB Furnace For 3-Dimensinal PSSM

$$\vec{v} = \left(\frac{Pe}{Pr}, 0, 0\right) \quad \text{at } 0 \le y \le 1 \ .\ 0 \le z \le 1 \qquad x = 0.B(y, z)$$

$$\text{at } = y = 0.1 \ .\ 0 \le z \le 1 \qquad 0 \le x \le B(y, z) \tag{7}$$

$$\text{at } = z = 0.1 \ .\ 0 \le y \le 1 \qquad 0 \le x \le B(y, z)$$

The boundary conditions for temperature and concentration at the interface are

$$[\vec{N}.\nabla T]_{\blacksquare} - Kc[\vec{N}.\nabla T]c = StPe[\vec{N}.\vec{e}_x] \quad (8)$$

$$[\vec{N}.\nabla C]_{\blacksquare} = \frac{PeSc}{Pr}(\vec{N}.\vec{e}_x)(1-k)C \quad (9)$$

Where $\vec{N}$ is unit normal vector to the interface as

$$\vec{N} = (\vec{e}_x - B_y\vec{e}_y - B_z\vec{e}_z)/\sqrt{1+B_y^2+B_z^2} \quad \text{and } B_y \equiv dB/dy,\ B_z \equiv dB/dz.$$

The thermal boundary condition at the wall is completely conducting to give

$$T = \frac{(10-x)}{10} \quad \text{at } 0 \le x \le 10 \ .\ 0 \le z \le 1, \quad y = 0,1$$

$$\text{at } 0 \le x \le 10 \ .\ 0 \le z \le 1, \quad z = 0,1 \quad (10)$$

$$T|_{x=0} = 1 \ , \ T|_{x=10} = 0 \quad (11)$$

The solute boundary condition at the entrance and at the wall are

$$[\vec{N}.\nabla C]_{\blacksquare} = \frac{PeSc}{Pr}(1-C) \quad (12)$$

$$\left.\frac{\partial C}{\partial y}\right|_{y=0,x=0} = \left.\frac{\partial C}{\partial y}\right|_{y=1,x=0} = \left.\frac{\partial C}{\partial z}\right|_{y=0,x=1} = \left.\frac{\partial C}{\partial z}\right|_{y=1,x=1} = 0 \quad (13)$$

$$\left.\frac{\partial T}{\partial y}\right|_{y=0,x=0} = \left.\frac{\partial T}{\partial y}\right|_{y=1,x=0} = \left.\frac{\partial T}{\partial z}\right|_{y=0,x=1} = \left.\frac{\partial T}{\partial z}\right|_{y=1,x=1} = 0 \quad (13)$$

Numerical Solution

The initial locations of the nodes are unchanged transversely and only the axial locations are coupled with the interface location to give the coordinate of the node as

Melt: $y_i = \dfrac{(i-1)}{(N_y-1)} \quad z_i = \dfrac{(j-1)}{(N_z-1)}$ (14)

$x_k \quad (k-1)\ B(y_{i,z})$ $\quad (N_{x,m}-1)$

Crystal: $y_i = \dfrac{(i-1)}{(N_y-1)} \quad z_i = \dfrac{(i-1)}{(N_z-1)}$ 15

$$x_k = B(y_i, z_j) + \frac{(k - N_{x,m})(\frac{L}{H} - B(y_i, z_i)}{N_{x,s}}$$

where N is the number of nodes in y-direction and N, is the number o1nodes in z-direction, and NA$ are the number of nodes axially in the melt and crystal respectively.

The shape of the melt/crystal interface is approximated by 2-dimensional biquadratic Lagrangian polynomials,

$$B(y,z) = \sum_{i=1}^{N_1} B^{(i)} \Phi^{i}(y,z) \qquad (16)$$

Where N is the number of nodes along the interface plane.

The Galerkin FEM and divergence theorem are applied to Eqs.(l)-(5) and (6) to yield residual equations as

$$\int_{D_m} [\Omega^i \bar{v}.\nabla\bar{v}^i + (\nabla.\Omega^i)p + \nabla.\bar{v} - \Omega^i GrT\,\bar{e_y}]\,dV = 0 \qquad (17)$$

$$\int_{D1} [\Omega^i \bar{v}. + (\nabla.\Omega^i)\,p + \nabla\Omega^i.\nabla\bar{v} - \Omega^i GrT\,\bar{e_y}]\,dV = 0 \qquad (18)$$

$$+ \int_{\partial D1} \phi^i \frac{Gr\,Sc}{Pr}(N.e_x)C(1-k)\,ds = 0 \qquad (19)$$

$$+ \int_{\partial D1} \phi^i\, StPe\,(\bar{N}.\bar{e_x})dS + \int_{\partial D1} \phi^i Bi(x)\,[T\infty(x) - T(x,y,z)\,dS = 0 \qquad (20)$$

The velocity, temperature, and concentration are approximated by twenty- seven—node Langrangian functions.

Pressure are

$$\begin{aligned} \psi^1(\xi,\eta,\zeta) &= 1 \\ \psi^2(\xi,\eta,\zeta) &= \xi \\ \psi^3(\xi,\eta,\zeta) &= \eta \\ \psi^4(\xi,\eta,\zeta) &= \zeta \end{aligned} \qquad (21)$$

The Jacobian matrix is 3 by 3, since the coordinate system is 3-dimensional and the mapping from global domain to local domain is given by

$$\begin{bmatrix} \frac{\partial\phi^i}{\partial x} \\ \frac{\partial\phi^i}{\partial\gamma} \\ \frac{\partial\phi^i}{\partial z} \end{bmatrix} = \begin{bmatrix} \frac{\partial x}{\partial\xi} & \frac{\partial\gamma}{\partial\xi} & \frac{\partial z}{\partial\xi} \\ \frac{\partial x}{\partial x} & \frac{\partial y}{\partial y} & \frac{\partial z}{\partial z} \\ \frac{\partial x}{\partial\xi} & \frac{\partial y}{\partial\xi} & \frac{\partial y}{\partial\xi} \end{bmatrix} \quad -i \begin{bmatrix} \frac{\partial\phi^i}{\partial\xi} \\ \frac{\partial\phi^i}{\partial\eta} \\ \frac{\partial\phi}{\partial\zeta} \end{bmatrix} = \bar{j}^{-1} \begin{bmatrix} \frac{\partial\phi^i}{\partial\xi} \\ \frac{\partial\phi^i}{\partial\eta} \\ \frac{\partial\phi}{\partial\zeta} \end{bmatrix} \qquad (22)$$

The relation of integration between the local and the global element is;

$$dx\ dy\ dz = |\bar{j}|\ d\xi\ d\eta\ d\zeta \qquad (23)$$

$$|\bar{j}| = \frac{\partial x}{\partial \xi}\left(\frac{\partial y}{\partial \eta}\frac{\partial z}{\partial \xi} - \frac{\partial z}{\partial \eta}\frac{\partial y}{\partial \xi}\right) + \frac{\partial y}{\partial \xi}\left(\frac{\partial z}{\partial \eta}\frac{\partial x}{\partial \xi} - \frac{\partial x}{\partial \eta}\frac{\partial x}{\partial \eta}\right) + \frac{\partial x}{\partial \xi}\left(\frac{\partial x}{\partial \eta}\frac{\partial y}{\partial \xi} - \frac{\partial y}{\partial \xi}\frac{\partial x}{\partial \xi}\right) \quad (24)$$

Gauss integration method is employed for the numerical integration in the finite element. The general form of numerical integration in 3dimensional finite element is

$$\int_{-1}^{1}\int_{-1}^{1}\int_{-1}^{1} f(\xi,\eta,\zeta)\, d\xi\, d\eta d\xi = \sum_{(i=1)(j=1)}^{\bar{m}}\sum^{\bar{m}}\sum_{(k=1)}^{\bar{m}} H_i\, H_i\, H_i\, f(\beta_i,\beta_i) \quad (25)$$

We employed m=3, that is corresponds to 3-point Gauss integration method. The residual equations for the interface location are formed by applying the Galerkin FEM to melting point constraint, Eq. (8) evaluated on the solid/melt interface as

$$\int_{\partial D_i} \phi_i(y,z)\, T\,(y,z,B(y,z) - T = (S)]\, dS = 0$$

where the differential unit of area element on the interface is

$$dS = \sqrt{1 + B_y^2 + B_z^2}\; dy\; dz$$

Results and Discussions

(1) Pe = 0.00281

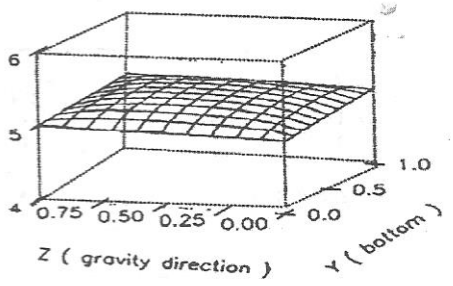

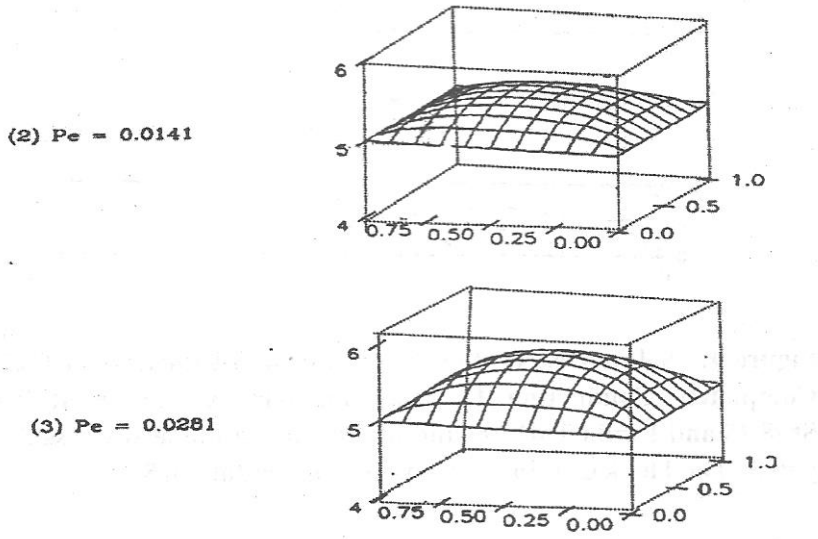

Figure 3: 3-D Interface Shape for Gr=0, Pr=0.059 Conducting Problem

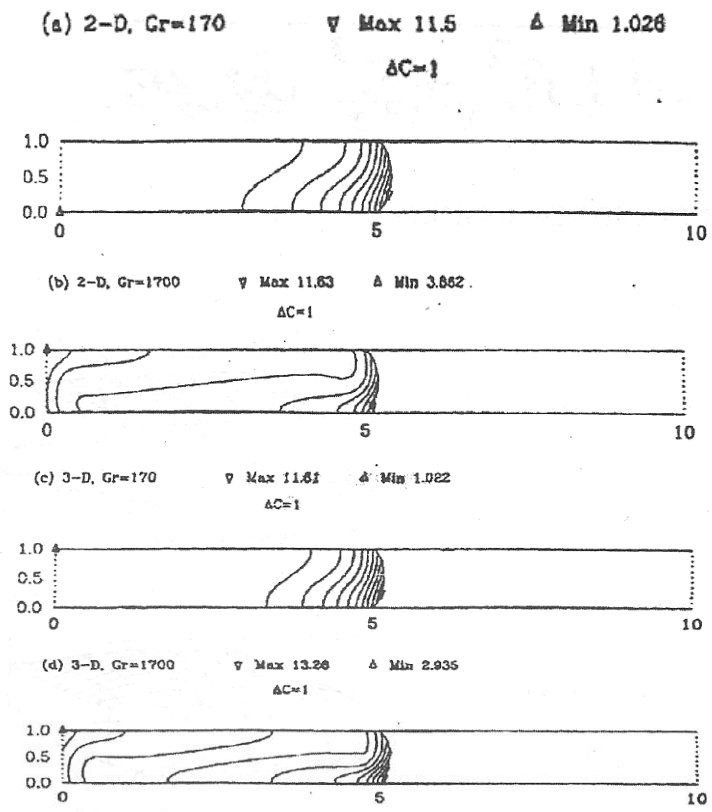

Figure 4: Solute Distribution Profiles from 3-Dimensional PSSM with Completely Conducting Thermal Boundary Condition at Pr=O.059, St8.25 and Pe=0.00281. (c) and (d) are in x-z Plane at Cross Section of y=O.5. The Thick Line in the Melt Phase is Contour of 5.

(a) Gr=0

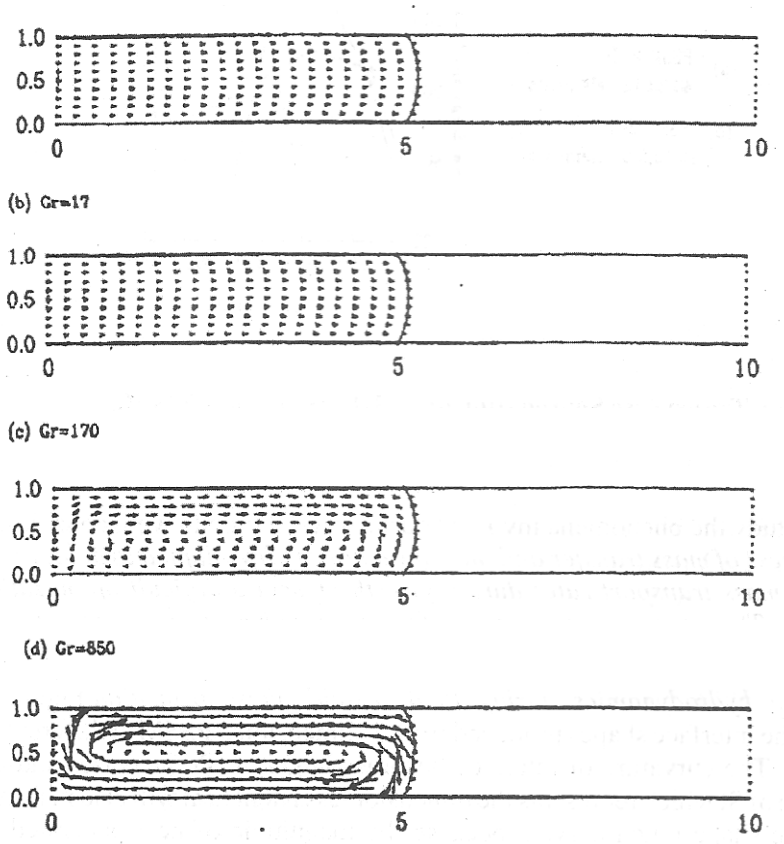

Figure 5: Flow Patterns at Various Cr Number from 3-Dimenisonal PSSM in x-z Plane at Cross Section of y=O.5.

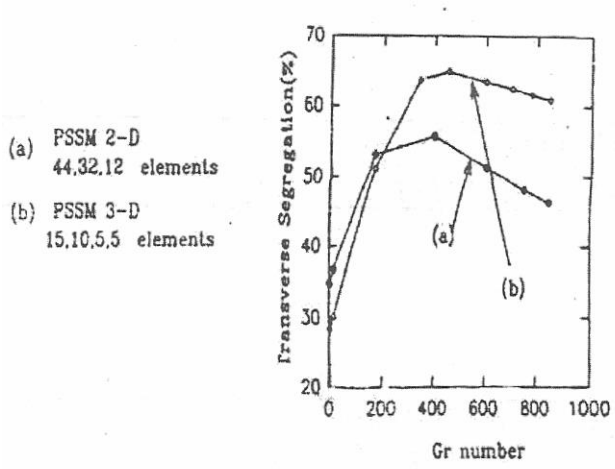

Figure 6: Transverse Segregation of 2-, 3-Dimensional PSSM at Pr=O.059, PeO.00281 and Sc=42.

In this study the phenomena involved during crystal growth were considered, the process of mass transfer and the convection modes adopted to achieve the desired mass

transport rates during growth present a difficult optimization problem. These transport processes affect the growth rate, crystal quality and the surface microstructure over the growing crystal faces.

As a result the science of crystal growth is governed by the principles of physiochemical hydrodynamics during fluid-to-solid phase transition. Figure 3. Shows the interface shapes produced from 3-dimensional PSSM at different Pe number. The curvature of interface becomes larger, as Pc increases and the increase of St which represents the dimensionless latent heat will also make the interface shape much curved, because the magnitude of heat generated by solidification is represented by Pe, St according to the previous boundary condition, Eq.(8). The thermal boundary condition is completely conducting one. The comparison of solution from two dimensional PSSM and 3- dimensional PSSM at cross section of y=O.5 is shown in Figure 4. In Figure 4.(b) and (d), the contours for dimensionless concentration of 5 is moved away from the interface region more . This is due to that the flow intensity is weaker in 3-dimensional case. At Gr=8), Umax of3-dimensional ease is 0.0141 mmlsec. The flow patterns at various Or are shown in Figure 5.Figure 6 shows the transverse segregation of 2-dimensional and 3-dimensional problem. In Figure 6, Or corresponding to the maximum;

Figure 6. Shows transverse segregation is less in 3-dimensional problem. The flow of 3-dimensional PSSM is less intense, and the curvature of interface of 3- dimensional PSSM is larger than that of 3-dimensional PSSM, so that the maximum point of transverse segregation appears later in 3-dimensional PSSM. At Gr=850, x(x_{max}, - X_{min} at interface) of 3-dimensional case is 0.384cm.

References

Arakawa, A. (1966). Computational design for long-term numerical integration of the equations of fluid motion; two-dimensional incompressible flow, Part 1, Journal of Computational Physics.1, 119-143.

Blagden, fl/K (2005). Monitoring Polymorphic Transformations in Solution. Journal of Superconductivity and Novel Magnetism. 12(4), 1207-1209.

Ciszek , T. F., Wang T.H. (2000). Silicon Float-Zone Crystal Growth as a Tool for the Study of Defects and Impurities. Presented at the Electrochemical Society, Fall Conference Phoenix, Arizona, October 22-27;

Ezema, F I. (2004). Fabrication, Optical Properties and Application of Undoped Chemical Bath Deposited ZnO Thin Film. Journal of Research (Science). l5,(4), 343-350.

Faister, R. (2012): Defect Control in Silicon Crystal Growth &Wafer Processing. Materials Science and Engineering 73 (20) .87-94.

Fang, H.S., Tian J., Wang s., Long Y., Zhang M.J & Zhao C. J. (2014). Numerical Optimization of Czochralski Sapphire Single Crystal Growth using Orthogonal Design Method. Crystal Research Technology, 49(7), 74 1-749.

Fang, H.S., Wang S., Jin Z.L., Tian J., & Xu J.F. (2013). Crystal Cracking Analysis and Three-Dimensional Effects during Kyropoulos Sapphire Growth. Crystal Research and Technology, 48(9), 649-657.

Fedyushkin, A. I. & Bourago, N.G. (2001). Influence of Vibrations on Boundary Layers. In Bridgman Crystal Growth. 2"Pan Pacific Basin Workshop on Microgravity Sciences paper CG 1073.

Fisher I . R, Shapiro,M. C & AnalytisJ. G. (2013). Principle of Crystal Growth of Intermetallic & Oxide Compound from Molten Solution.

Grishechkin, Y. A. & Kapshai, V.N. (2014). Coupled S-States of Relativistic Two-Particle systems with Energy Dependent Single Boson Exchange Potentials. Russian Physics journal, 12, 79-85.

Hossain, M. A., Paul, S. C., Mandal, A. C., (2002). Natural convection flow along a vertical circular cone with uniform surface temperature and surface heat flux in a thermally stratified medium, Int. J. Numer. Methods Heat and Fluid Flow, 12, 290-305.

Hung, H. (2009). Epitaxial Crystal Growth. Proceedings of Algorithm. 196-201.

Kakimoto, K. (2013). Development of Crystal Growth Technique of Silicon by the Czochraslski Method. Journal of Acta physicapolonica. 124(2), 227-230.

Lin, F. N., (1976). Laminar convection from a vertical cone with uniform surface heat flux, Letters Heat Mass Transfer, 3,49-58.

Nollet, S. Hilger C. & Urai, J .L (2006). Experimental Study of Pollycrystal Growth for an Advecting Supersaturated Fluid in a Model Fracture. Geofluid 6, 185-200.

Qubbaj, A .R , Gollahalli, S ,R. & Villareal , J (2002). Numerical Modeling of a Turbulent gas Jet Flame in a Swirling Air Stream; America Society of Mechanical Engineers (ASME) Proceeding Combustion and Alternative Energy.

Riedi, N. & Wendrock, K. L. (2014). The Reliability of High Resolution Electron Backscatter Diffraction Determination of Strain and Rotation Variation using Phase-Only and Cross Correlation. *Journal of Low Temperature Physics*. 175(3-4), 580-589.

Roque S. S. Regina CC. M., Maria M.R.A. Lima, Bogdan A. Sava. Mihali E. (2014). Phase Transformation and Microstructure Evolution after Heat Treatment of a Terbium-Doped Lithium-Aluminum phosphate glass. Journal of Material Science, 49(13), 4601-4611.

Shockely, M. (1993). Theoretical Background of Single Crystal Growth and its Applications. Workshops in Korea.

Scheil, E. (1942). Bernerkungen zur Schichtkristallbildung, Metallkde., 34, 70-72.

Sze, S.M. (1985). Semiconductor Devices: Physics and Technology, Second Edition. John Wiley & Sons, New York.

Wang W. & Hu W.R (2010). Concentration Distribution in Solution Crystal Growth: Effect of Moving Interface Conditions. *Journal of Crystal Growth* 403,227-233.

Wang, W.Lee H. K., Kim G.W. (2(I3). Crystal Growth Structure and Spectroscopic Studies of a Novel Organic Single Crystal. Crystal Research & Technology, 41(3), 204-211.